JOURNAL OF MATERIALS SCIENCE 26 (1991) 99–102

# A map for wear mechanisms in aluminium alloys

Y. LIU, R. ASTHANA, P. ROHATGI
*Materials Department, University of Wisconsin–Milwaukee, Milwaukee, Wisconsin 53201, USA*

A quantitative wear map for aluminium and its alloys has been constructed using normalized test variables and the physical modelling approach proposed by Lim and Ashby for steels. New model equations based on a different state-of-stress criterion suitable for aluminium alloys have been developed and found to match well with reported experimental wear data on aluminium alloys. The field boundaries between various interfacing wear mechanisms were constructed by using critical values of experimental wear data which manifest themselves in discontinuities in the slope of wear curves. However, within a given wear regime, the model equations developed here agreed fairly well with the reported wear data. The wear mechanisms successfully modelled here include oxidation dominated wear, delamination wear, severe plastic deformation wear, and melt wear.

## 1. Introduction

Following an initial suggestion by Tabor [1], Lim and Ashby [2] constructed the first wear mechanism maps based on physical modelling in order to systematize empirical wear data on steels. These maps allowed prediction of dominant wear mechanisms under a given set of test conditions in terms of a few key dimensionless parameters, and of how various mechanisms of wear interface with one another.

In this paper a wear mechanism map for aluminium alloys is presented, based on the physical modelling approach suggested by Lim and Ashby [2]. A qualitative map to organize wear data on aluminium alloys was presented recently by Antoniou and Subramanian [3]. Here new model equations based on a different state-of-stress criterion suitable for aluminium and its alloys have been developed and calibrated with the help of available experimental data. The various symbols and the normalized parameters (pressure, velocity, wear rate) used here are the same as those used by Lim and Ashby [2]. The predictive capability of these wear maps can be improved by invoking more realistic physical models of wear and by generating more reliable and reproducible data. Finally these maps can also be constructed to encompass new-generation tailor-made engineering materials such as metal-matrix composites which may have potential as future tribological materials.

## 2. Wear models and their calibration

### 2.1. Oxidation-dominated wear

At relatively low sliding speeds and normal loads the frictional heat generated at contacting asperities forms an oxide layer on aluminium at the sliding surface. Initially this oxide layer is thin and it deforms elastically. Almost no wear debris is generated during this stage which is also termed extra-mild wear. With increasing normal loads, adhesion between the steel disc and surface oxide film effects material removal in the form of laminar particles of average size 50 to 200 μm. The principal chemical components of this type of wear debris have been reported to be iron, silicon and $\alpha/\gamma\ Al_2O_3$ [4, 5].

Lim and Ashby [2] presented a model of oxidation wear of iron alloys where, like aluminium alloys, the oxidation kinetics are parabolic [6]. These authors considered contacting asperities at the sliding surface to be plastic and, therefore, assumed $F = A_r H_0$, where $A_r$ is the local asperity contact area; $F$ is the normal force on sliding surface; $H_0$, hardness; $K$, a constant dependent on the material properties and $A_n$, nominal area of contact. For aluminium alloys, however, a more realistic assumption substantiated with experiments [7, 8] is to consider elastic deformation at asperities, especially those in the oxidation layer, during oxidation dominated wear. In this case, equilibrium requires [9] that $A_r = KF^{2/3}$ or, in terms of normalized pressure

$$A_r = \bar{F}^{2/3} K (H_0 A_n)^{2/3} \quad (1)$$

where $K$ is a material constant.

Substituting for $A_r$ from Equation 1 in the expression for oxidation-dominated wear rate (equation 31 of [2]), the normalized wear rate, $\bar{W}$, for aluminium alloys is obtained as

$$\bar{W} = \left(\frac{C^2 A_0 K r_0}{a Z_c}\right)\left(\frac{H_0}{A_n}\right)^{1/3}\left(\frac{\bar{F}^{2/3}}{\bar{V}}\right)\exp\left(\frac{-Q_0}{RT_f}\right) \quad (2)$$

where $T_f$ is the flash temperature; $C$ the constant used in the model of oxidation dominated wear; $r_0$, the radius of the bearing pin; $a$, thermal diffusitivity of the metal; $Z_c$, the critical thickness of the oxide film; $V$, sliding velocity and $R$ is the gas constant.

0022–2461/91 $03.00 + .12 

The Arrhenius constant, $A_0$, and the activation energy, $Q_0$, for oxidation can be considered as adjustable parameters [2] because considerable difference exists between the dynamic process of oxidation wear under severe mechanical loading, and the standard, static oxidation tests that are used to obtain handbook values of $A_0$ and $Q_0$. The oxidation rate constant, $K_p$, for the growth of an alumina layer at 600 °C is reported by Geiger and Poirier [6] to be $\sim 8.5 \times 10^{-14}\,\mathrm{kg^2\,m^{-4}\,sec^{-1}}$, who also note several orders of magnitude scatter in the $K_p$ values for aluminium oxide. We have chosen $Q_0 = 121\,\mathrm{kJ\,mol^{-1}}$ and $A_0$ as given later.

An expression can now be derived for the number, $N$, of contacting asperities under elastic rather than plastic conditions, by integrating the differential equation relating $N$ to $(A_r/A_n)$ (cf. Appendix I in [2]). Using the limit $N = 1$ at $(A_r/A_n) = 1$ and substituting for $A_r$ from Equation 1 in the resulting expression, we obtain the following equation for $N$

$$N = \left(\frac{r_0}{r_a}\right)^2 \bar{F}^{2/3} K \left(\frac{H_0}{A_n}\right)^{2/3} \times \left[1 - \left(\frac{K^{3/2} H_0 \bar{F}}{A_n^{1/2}}\right)^2\right] + 1 \qquad (3)$$

Using the result $(N\pi r_a^2/\pi r_0^2) = (A_r/A_n)$; Equation 3 can be rewritten as

$$\left(\frac{A_r}{A_n}\right) = K\bar{F}^{2/3}\left(\frac{H_0}{A_n^{1/2}}\right)^{2/3} \times \left[1 - \left(\frac{K^{2/3} H_0 \bar{F}}{A_n^{1/2}}\right)^2\right] + 1 \qquad (4)$$

Now, using the data from [10] on fractional area contacted $(A_r/A_n)$ against $\bar{F}$ for the aluminium–duralumin system in Equation 4, the material constant $K$ is found to vary in the range $10^{-5}$ to $10^{-6}$. A value of $5 \times 10^{-6}$ is used for $K$ which is also taken as roughly representative of the aluminium–steel system in the absence of pertinent data on that system.

The expression for flash temperature, $T_f$, which is required in Equation 2 for $\bar{W}$ is obtained by modifying equation 14 of Lim and Ashby [2] to take account of elastic rather than plastic deformation conditions expected to prevail [7, 8] at contacting asperities. By substituting for $(r_a/r_0)$ from Equation 3 in equation 14 of [2], the modified expression for $T_f$ is obtained as

$$T_f = T_b + \frac{\alpha\mu T^* \beta \bar{V} K^{1/2} \bar{F}^{1/3}}{N^{1/2} r_0} (H_0 r_0^2)^{1/3} \qquad (5)$$

where $\mu$ is the coefficient of friction and the bulk temperature, $T_b$, is given by equation 8 of [2], and $N$ is given by Equation 3 derived earlier. Here $\beta^* \simeq 1.0$, $\mu = 0.40$ [4, 11, 12], $T_0 = 298$ K, $T^* \simeq 116$ K for aluminium. A complete list of material constants for aluminium used in the present calculations is given in Table I. The heat distribution coefficient, $\alpha$, in Equation 5 was obtained from equation 6 of [2] as 0.12 to 0.34 for the range of $\bar{V}$ (1 to $10^2$) of interest in the oxidation wear regime of aluminium.

TABLE I Material constants for aluminium

| | |
|---|---|
| $T_m$ | 933 K |
| $T_0$ | 298 K |
| $T^*$ | $\simeq aH_0/K = 116$ K |
| $L$ | $397.1 \times 10^3\,\mathrm{J\,kg^{-1}}$ |
| $H_0$ | $30 \times 10^7\,\mathrm{N\,m^{-2}}$ |
| $r_0$ | $3 \times 10^{-3}$ m |
| $r_a$ | $10^{-5}$ m |
| $C$ | $2.34 \times 10^{-4}(3M_{Al}/4M_O\rho_{Al})$ |
| $M_{Al}$ | 27 |
| $M_O$ | 32 |
| $\rho_{Al}$ | $2705\,\mathrm{kg\,m^{-3}}$ |
| $Z_c$ | $\simeq 20 \times 10^{-6}$ m [9] |
| $K_m$ | $234\,\mathrm{W\,m^{-1}\,K^{-1}}$ |
| $C$ | $900\,\mathrm{J\,kg^{-1}\,K^{-1}}$ |
| $a$ | $9.61 \times 10^{-5}\,\mathrm{m^2\,sec^{-1}}$ |
| $Q_0$ | $\simeq 121\,\mathrm{kJ\,mol^{-1}}$ |

The (empirical) Arrhenius constant, $A_0$, is obtained by substituting Equations 3, 5 and the expression for $T_b$ (from equation 8 of [2]) into Equation 2 to yield an expression for $\bar{W}$ in terms of $\bar{F}$ and $\bar{V}$. The experimental measurements on wear rate of pure aluminium from [12] were used in this expression for $\bar{W}$ to evaluate $A_0$ which was obtained as $7.96 \times 10^{16}\,\mathrm{kg^2\,m^{-4}\,sec^{-1}}$.

Finally, using Equation 2, contours of constant normalized wear rates for oxidation-dominated wear of aluminium were constructed as shown in Fig. 1. Superimposed on Fig. 1 are experimental data from several sources. A good quantitative agreement between model equations and empirical data is noted in this wear regime.

## 2.2. Delamination wear

Delamination wear or plasticity dominated wear involves plastic shearing of metal in the sliding direction. Suh [13], among others, has proposed a widely accepted theory of delamination wear based on fracture mechanics which considers nucleation of subsurface cracks due to plastic shearing on the sliding surface. These subsurface cracks propagate under combined frictional shear stresses and the normal surface adhesion stresses, and eventually break open to give particle-like wear debris. Based on Suh's equation [13], the wear volume, $\Delta V$, is related to normal load, $F$, and the sliding distance, $S$, by $\Delta V = K_1 F \Delta S$, where $K_1$ is a complex function of stress state and material properties. The wear rate $W = \Delta V/\Delta S = K_1 F/S_c$, where $S_c$ is a critical sliding distance. For aluminium and other soft alloys, $W$ is not only a function of load but also of sliding speed $V$ [8, 11, 13, 14], so that, assuming $S_c = K_2 V$ where $K_2$ is a material constant, we obtain $W = K_0 F/V$, or in terms of normalized variables

$$\bar{W} = \left(\frac{K_0 H_0 r_0}{a}\right) \bar{F}/\bar{V} = K_3 \bar{F}/\bar{V} \qquad (6)$$

The constant $K_3$ in Equation 6 is a complex function of several factors including alloy composition. It is well known that content, size and spatial distribution

*$\beta$ is a dimensionless number and represents the ratio of linear heat diffusion distance to the radius of the bearing pin.

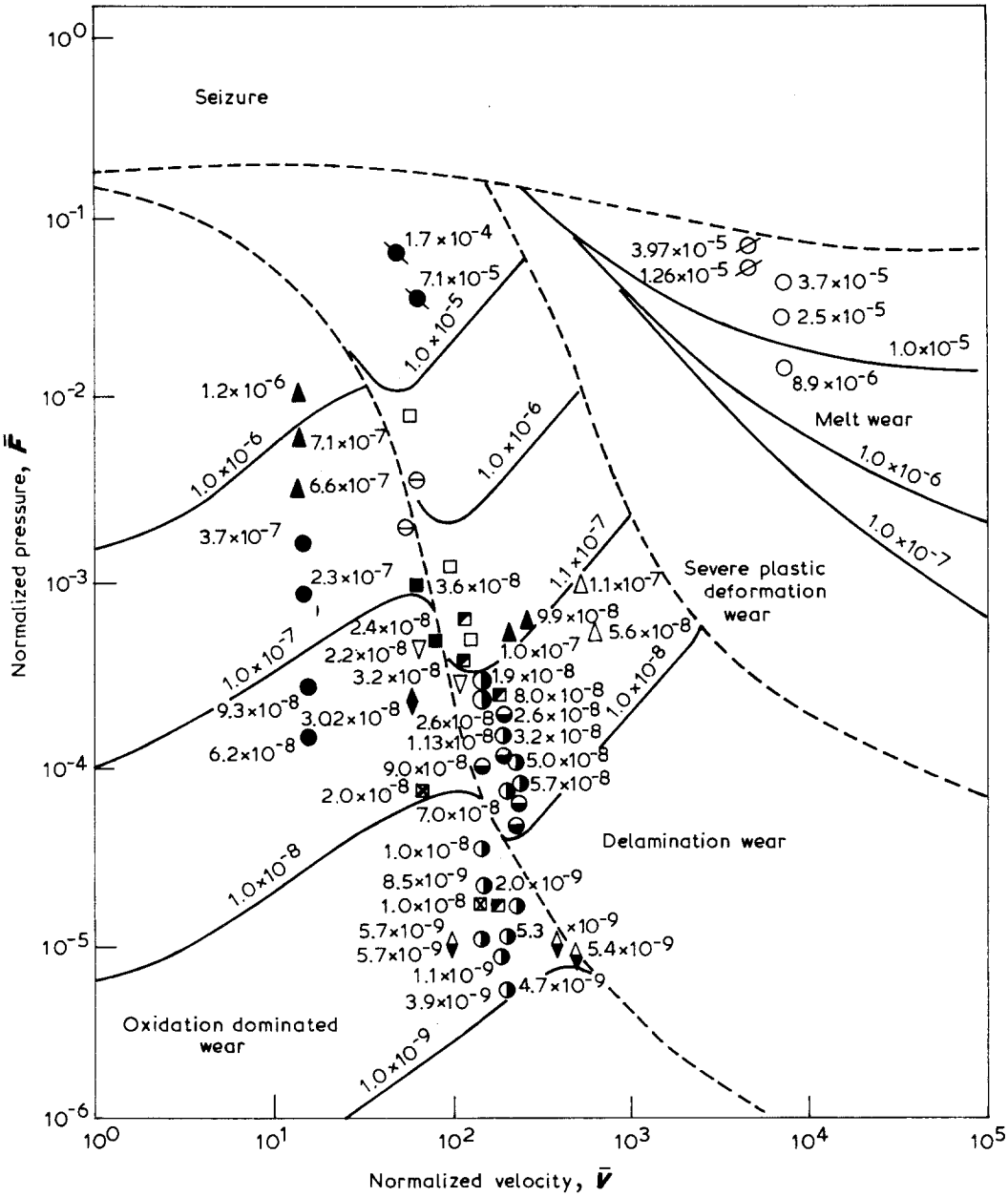


*Figure 1* A map for wear mechanisms in aluminium alloys. (⊗) [4], (◒) [7], (◆, ◑ ⊠) [17], (●) [15], (ϕ) [20], (◆) [14], (▽, ◩) [5], (□) [18], (▲) [12], (○) [16], (●) [19], (△) [21]. The numbers in the figure represent normalized wear rate, $\bar{W} = W/A_n$, where $W$ is the wear rate in $m^3 m^{-1}$ and $A_n(m^2)$ is the nominal area of contact.

of silicon in Al–Si alloys have an effect on wear rate under dry sliding conditions [5, 9, 15]. The wear data on Al–Si alloys from [5] and [12] were used to calibrate the constant $K_3$ of Equation 6. A plot of $K_3$ against silicon content showed an increase in the value of $K_3$ with silicon especially in the hypereutectic composition range. $K_3$ was typically taken as $5 \times 10^{-2}$ for calculations. The constant wear rate contours based on Equation 6 for plasticity dominated wear and the empirical wear data on several Al–Si alloys from various studies are shown in Fig. 1 and a fair agreement can be noted between the two.

## 2.3. Melt lubrication wear

Melt lubrication wear broadly refers to surface heating and mass transfer from the aluminium surface to a harder substrate such as a steel disc at relatively high speeds and high loads, regardless of whether or not surface melting accompanies material removal. If, however, surface melting does occur at high sliding speeds, as in projectile-type impact wear tests, the ejection or extrusion of the melt becomes the dominant mode of material removal. This process is characterized by a sharply reduced coefficient of friction (0.2 to 0.02) as a result of reduced viscosity of the extruded molten layer.

Alternatively, μ may be reduced less drastically during high-speed wear tests indicating that gross mass transfer due to severe plastic deformation rather than surface melting is the dominant mode of material removal in this type of wear processes.

The following normalized wear rate equation for melt wear has been proposed [2]

$$\bar{W} = \frac{(T_m - T_0)}{T^*}\left(\frac{H_0}{L}\right) \times \left(\frac{K_a}{\beta \bar{V}}\right)\left[\alpha\mu\bar{F}\bar{V}\frac{T^*\beta}{(T_m - T_0)} - 1\right] \quad (7)$$

where the constant $K_a$ was taken as unity in [2], assuming that all the metal which melts is ejected. However, we have assumed $K_a < 1$ to account for the fact that only a fraction of the molten volume will be squirted out while the rest would flow over the cooler areas on the surface and resolidify. In the Equation 7, $\mu \simeq 0.14$ and the latent heat, $L \equiv 397.1 \times 10^3\ \mathrm{J\,kg^{-1}}$. The adjustable constant $K_a$ in Equation 7 was calibrated by using experimental data on melt lubrication wear of aluminium from [16] and found to be $10^{-5}$ to $10^{-6}$ in the region of interest in the neighbourhood of $\bar{F} \sim 10^{-2}$ for the melt wear regime. Although the experimental data on melt wear of aluminium alloys are scarce, the constant wear rate contours calculated from Equation 7 agree well with the results of the two experimental studies on melt wear of aluminium reported in the literature (see Fig. 1).

In the case of severe plastic deformation wear, the frictional heating at contacting asperities leads to plastic flow of metal and the friction coefficient drops somewhat less sharply. Energetically, the frictional heat flux is partitioned between the bearing pin and the contact points. The energy for plastic flow is [7]

$$E_{\mathrm{def}} = \frac{K' F h A_Q}{A_n} \tag{8}$$

where $h$ is the depth of mass flow, $A_Q$ is the area of plastically deformed layer, and $K'$ is a constant. If the worn volume is assumed to be $V_m = CA_Q h$ then $W = V_m/VA_n = ChA_Q/VA_n$. The equilibrium heat balance, therefore, requires

$$\frac{\alpha \mu F V}{A_n} = \frac{K_m(T_f - T_0)}{l_b} + \frac{K' F h A}{A_n}$$

where $K_m$ is thermal conductivity of metal. This expression can be rearranged to obtain $\bar{W}$ as defined above

$$\bar{W} = \frac{(T_f - T_0)}{K' A_n T^* \bar{F} \bar{V}} \left( \frac{\alpha \mu \bar{F} \bar{V} T^*}{T_f - T_0} - 1 \right) \tag{9}$$

Here, both $T_f$ and $\mu$ are functions of sliding speed. Unfortunately, empirical wear data on aluminium in this wear regime are not available and, therefore, constant $K'$ in Equation 9 could not be calibrated. Nevertheless, the field boundary for this wear regime is schematically shown in Fig. 1 as a narrow band.

### 2.4. Seizure

During seizure, the local asperity contact area, $A_r$, grows by plastic deformation under normal load to accommodate the applied load, and complete seizing occurs when $A_r = A_n$. The seizure equation derived by Lim and Ashby (equation 22 in [2]) has been used to plot seizure line for aluminium alloys with $\alpha_t = 12.0$, $\mu = 1.0$, $T_m = 933$ K and $T_b$ given by equation 8 of [2]. Due to unavailability of experimental seizure data on aluminium alloys, the theoretical curve could not be tested against data. The field boundaries between various interfacing mechanisms were constructed empirically by plotting critical data points from several sources (i.e. points at which wear curves showed discontinuous changes in the slope). The overall agreement between experimental data and model equations appears to be fair.

## 3. Conclusions

An attempt has been made to construct a wear mechanism map for aluminium alloys by using normalized test variables and models of wear. Only a few recent references (listed below) were used to construct the wear map presented here, although over sixty papers dealing with the wear of aluminium alloys were used as a basis for the classification of wear mechanisms that have been assumed here.

The agreement between theory and experimental data appears to be fair within a given wear regime and quantitative predictions of wear rate can be made. Refinements in the models of wear and generation of more accurate and reproducible data can improve practical utility of these maps which can be extended to new engineering materials such as metal-matrix composites.

## References


1. D. TABOR, in "New Directions in Lubrication, Materials, Wear and Surface Interactions", edited by W. R. Loomis (Noyes, Park Ridge, New Jersey, USA, 1985) p. 1.
2. S. C. LIM and M. F. ASHBY, *Acta Metall.* **35** (1987) 1.
3. R. ANTONIOU and C. SUBRAMANIAN, *Scripta Metall.* **22** (1988) 809.
4. K. RAZAVIZADEH and T. S. EYRE, *Wear* **79** (1982) 325.
5. A. D. SARKAR and J. CLARKE, *ibid.* **75** (1982) 71.
6. G. M. GEIGER and D. R. POIRIER, "Transport Phenomena in Metallurgy" (Addison-Wesley, Menlo Park, California, 1980).
7. K. MOHAMMAD JASIM and E. S. DWARKADASA, *ibid.* **119** (1987) 119.
8. P. K. ROHATGI, Y. LIU and T. L. BARR, unpublished research (1989).
9. F. P. BOWDEN and D. TABOR, "The Friction and Lubrication of Solids", Parts I and II (Butterworth, London, 1950 and 1964).
10. P. B. MADAKSON, *Wear* **87** (1983) 191.
11. P. K. ROHATGI, N. B. DAHOTRE, Y. LIU and T. L. BARR, in "Wear Resistance of Metals and Alloys", edited by G. R. Kingsbury (American Society for Metal, Metals Park, Ohio, 1988) p. 47.
12. B. N. PRAMILLA BAI and S. K. BISWAS, *Wear* **120** (1987) 61.
13. N. P. SUH, *ibid.* **25** (1973) 111.
14. R. ANTONIOU and D. W. BORLAND, *Mater. Sci. Engng* **93** (1987) 57.
15. R. SHIVNATH, B. K. SENGUPTA and T. S. EYRE, *Brit. Foundrymen* **70** (1977) 349.
16. B. STERNLICHT and M. APKARIAN, *ASLE Trans.* **2** (1959) 248.
17. K. MOHAMMAD JASIM and E. S. DWARKADASA, *Wear* **82** (1982) 377.
18. J. CLARKE and A. D. SARKAR, *ibid.* **69** (1981) 1.
19. B. N. PRAMILLA BAI and S. K. BISWAS, *ASLE Trans.* **29** (1986) 116.
20. R. S. MONTGOMERY, *Wear* **38** (1976) 235.
21. C. BEESLEY and T. S. EYRE, *Tribology Int.* **9** (1976) 63.



*Received 19 July*
*and accepted 22 November 1989*